Supporting Information

Spectroscopically Quantifying the Influence of Salts on Non-Ionic Surfactant Chemical Potentials and Micelle Formation

Denilson Mendes de Oliveira and Dor Ben-Amotz*

Department of Chemistry, Purdue University, West Lafayette, IN, USA

*Email: bendor@purdue.edu

The following supplementary materials are provided in this document:

1. Experimental Methods
2. Additional Experimental Results
   (a) Raman-MCR SC spectra of 12HD in aqueous 0.25 M Na_2SO_4 and aqueous 2 M NaSCN (Fig. S1)
   (b) Perturbation of the C≡N vibrational mode by 12HD in aqueous 0.5 M (Fig. S2) and 2 M NaSCN (Fig. S3)
   (c) Lack of perturbation of the S=O vibrational mode by 12HD in 0.25 M aqueous Na_2SO_4 (Fig. S4)
3. Derivation of Micellization and Wyman-Tanford Expressions
4. Wyman-Tanford Partition Coefficient Bounds

1 Experimental Methods

Aqueous solutions of 12HD (1,2-hexanediol, Sigma-Aldrich, 98%), NaSCN (sodium thiocyanate, Sigma-Aldrich, $\geq$ 98%), and Na_2SO_4 (sodium sulfate, Sigma-Aldrich, $\geq$ 99%) were prepared with ultrapure filtered water (Milli-Q UF Plus, Millipore, 18.2 MΩ cm). Raman spectra were obtained at 20°C using an Ar-ion 514.5 nm laser with $\sim$20 mW of power at the sample and 5 min of integration time. Backscattered Raman photons were collected from the sample using a 20$\times$ long-working-distance microscope objective (NA = 0.42, Mitutoyo Inc.) and transmitted with an optical fiber to an imaging spectrograph (SpectraPro300i, Acton Research Inc.) that was equipped with a 300 grooves/mm grating and a thermoelectrically cooled CCD camera (Princeton Instruments Inc.).

Self-modeling curve resolution (SMCR) was performed with pairs of solvent and solution spectra to obtain Raman-MCR solute-correlated (SC) spectra[1–4]. In these spectral decompositions, the solvent spectrum was constrained to either being pure water or the corresponding salt solution. Thus, the SC spectra include vibrational bands arising from 12HD as well as features arising from solvent molecules whose vibrational spectra are perturbed by 12HD. So, when the solvent is a salt solution, the SC spectra may include features arising from 12HD-induced perturbation of the vibrational spectra of both the water and the salt molecular anions (SCN^- or SO_4^{2-}).

Monomer and aggregate concentrations of 12HD were estimated using total least squares (TLS) regression.[5,6] In this procedure, the SC spectrum of a given 12HD solution is decomposed into a linear combination of free and aggregated components, obtained as follows: (i) the monomer spectrum is the SC spectrum of a sufficiently dilute solution of 12HD so that no aggregation has taken place; and (ii) the aggregate spectrum is obtained from a second round SMCR analysis performed on the first round SC spectra obtained at different 12HD concentrations.

The critical micelle concentration (C_A) was obtained from a plot of the resulting (TLS derived) monomer and aggregate concentrations as a function of the total surfactant concentration $[12HD]_T$. The C_A value was identified as the x-axis intercept of a linear fit to the concentration of aggregated 12HD as a function $[12HD]_T$, performed over a concentration range from 0.7 M to 2 M, which is well above C_A, as further described in the parent manuscript.

2 Additional Experimental Results

Figure S1 compares the free monomer (solid curves) and micelle (dotted curves) SC spectra of 12HD in pure water (blue), aqueous 0.25 M Na_2SO_4 (green), and aqueous 2 M NaSCN (red). Note that both the free monomer and micelle hydration shell spectra of 12HD in aqueous Na_2SO_4 are quite similar to those in pure water. This indicates that there is little direct interaction between either Na^+ or SO_4^{2-} and 12HD, although the small influence of this salt on the micelle hydration shell spectrum may indicate the slight penetration of SO_4^{2-} ions into the hydration shell of the micelle. In aqueous NaSCN, on the other hand, both the free monomer and micelle spectra are significantly different than those in pure water, thus indicating the significant interaction between SCN^- ions and the hydration shells of both the free monomers and micelles. The decrease in the OH band area of the free monomer in aqueous NaSCN is consistent with the penetration of SCN^- into the first hydration shell of 12HD, thus expelling some water molecules out to the surrounding solvent. The increase in area of the micelle hydration shell spectrum in aqueous NaSCN implies that interactions between the SCN^- ions and the micelle alters the micelle hydration sphere water structure, relative to that of the hydration sphere of a micelle in pure water.

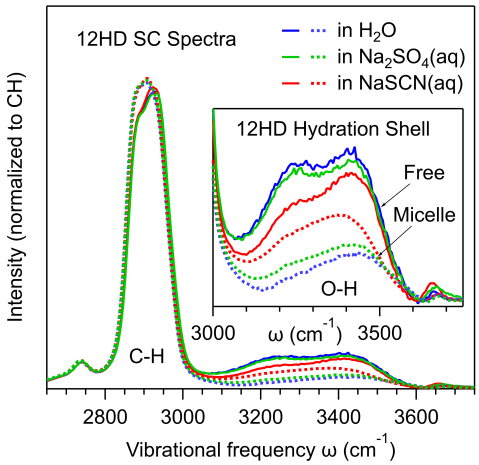

Figure S1. Raman-MCR SC spectra of free (solid curves) and aggregated (dotted curves) 12HD in pure water (blue), aqueous 0.25 M Na_2SO_4 (green), and aqueous 2 M NaSCN (red).

It is also noteworthy that in all the solutions the hydration shell band of the free monomer has a more prominent shoulder near 3200 cm^{-1}, relative to that in pure water. An increase in the 3200 cm^{-1} shoulder implies an increase tetrahedral ordering in the hydration shell of the free monomer,

as is the case in the hydration shell of other alcohols,[7,8] as well as methane,[9] dissolved in water. On the other hand, the hydration shell OH band of the micelle has a less prominent 3200 cm^{-1} shoulder and is shifted to higher frequency (relative to the monomer hydration shell) thus indicating that the micelle hydration shell is less ordered (and more weakly hydrogen-bonded) than the hydration shell of the free monomer, as is also the case in other concentrated (crowded) aqueous alcohol solutions.[10] Moreover, the smaller area of the micelle hydration shell band is consistent with the aggregation-induced expulsion of water molecules from the oily tails of some of the 12HD molecules, as also observed in other micelle Raman-MCR spectra.[11]

Further evidence of the interaction between SCN^- and 12HD is provided by the spectra shown in Fig. S2, which compares the C≡N stretch band features that appear in aqueous NaSCN (dashed black curve) with those in the 12HD SC spectra (solid curves). Comparison of the dashed black and high concentration solid purple curve clearly reveals that the interaction between SCN^- and the micelles produces a significant red-shift in the C≡N stretch band of SCN^-. At the lowest 12HD concentrations, the C≡N stretch band appears to split into two sub-bands. A clue regarding the assignment of these sub-bands is provided by additional measurements, performed in aqueous solutions with a lower NaSCN concentration of 0.5 M, in which the free monomer SC spectrum has a single C≡N band that is blue-shifted relative to the C≡N of aqueous NaSCN, as shown in Fig. S3.

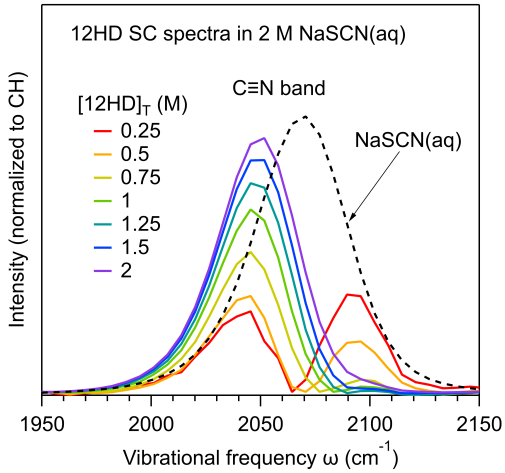

Figure S2. The SC C≡N stretch band of aqueous 2 M NaSCN (dashed black curve) is compared with the C≡N bands appearing in the concentration dependent SC spectra of 12HD.

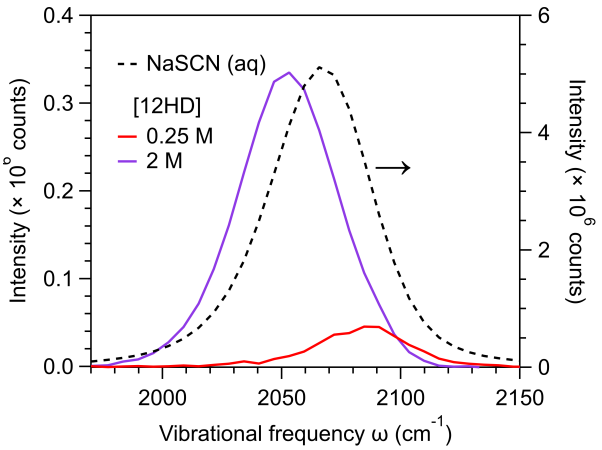

Figure S3. The C≡N band in aqueous NaSCN (dashed-black band) is compared with that in the SC spectrum of 12HD dissolved in 0.5 M NaSCN. Note that interaction of SCN^- with 12HD monomers at low concentration shifts the C≡N band to higher frequency, while the interaction of SCN^- with 12HD micelles at high concentration shifts the C≡N band to lower frequency.

Thus, the two bands in the red (and orange) spectrum in Fig. S2 are apparently due to SCN^- ions interacting both with free 12HD monomers and with some low order aggregates of 12HD. Note that the red bands pertain to a 12HD concentration of 0.25 M, which is well below C_A and so there should be virtually no micelles in this solution, but there may be some lower order aggregates of 12HD. Thus, the appearance of a low frequency C≡N sub-band in Fig S2 at 12HD concentrations down to 0.25 M indicates that low order aggregates of 12HD are stabilized in 2 M NaSCN. It is also important to note that the appearance of two bands in a SC spectrum can also arise when a single hydration shell band is broader than the corresponding solvent band,[12] and so the two red (and orange) bands in Fig. S2 could also arise from a single broad hydration shell C≡N band, resulting from a distribution of 12HD monomers and small aggregates.

The fact that the strongly kosmotropic anion SO_4^{2-} is expelled from the hydration shell of 12HD is evidenced not only by the similarity of the free monomer hydration shell spectra in pure water and aqueous Na_2SO_4 (Fig. S1), but also by the fact that the S=O stretch band of SO_4^{2-} is not perturbed by 12HD, and thus does not appear in the SC spectra of 12HD (see SI Fig. S3). This absence of an S=O band in the SC spectrum of 12HD at all concentrations implies that sulfate ions are expelled from both the monomer and micelle hydration shells.

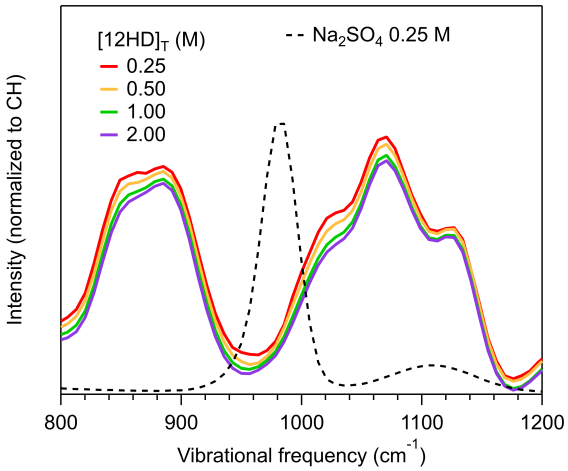

Figure S4. The S=O band in aqueous Na_2SO_4 (dashed-black band) is compared with that in the SC spectrum of 12HD dissolved in 0.25 M Na_2SO_4. Note that the solid curves reveal bands due to 12HD (normalized to the same CH band area), and show no evidence of a perturbed S=O band, thus confirming that there is no indication of any interaction between SO_4^{2-} and either the free monomers or micelles of 12HD.

3 Derivation of Micellization and Wyman-Tanford Expressions

The formation of micelles in an aqueous solution is driven by the equilibrium between free surfactant monomers (M) and micelle aggregates (M_n) of size n, dictated by the following difference between the corresponding chemical potentials.[13]

$$\Delta\mu_n^\circ = \mu_n^\circ - \mu_1^\circ \tag{1}$$

Note that μ_i° is the chemical potential of a monomer in an aggregate of size i at a standard state concentration of $C_i = 1\,\mathrm{M}$, and C_i is the total concentration of monomers that reside in an aggregate of size i. If the concentrations remain sufficiently low that interactions between free monomers and micelles may be neglected, the concentrations may be equated with the corresponding activities. Under these conditions, the micelle formation equilibrium constant, $K_n = [M_n]/[M]^n = (C_n/n)/C_1^n = e^{-\beta n \Delta\mu_n^\circ}$, will be approximately independent of the total surfactant concentration (and if the chemical potentials are expressed in molar units, then $\beta = 1/RT$, where T is the absolute temperature and R is the gas constant). Thus, Eq. 2 may be used to relate

the aggregated and free monomer concentrations.[13]

$$C_n = n\left(C_1 e^{-\beta\Delta\mu_n^\circ}\right)^n \tag{2}$$

Equation 2 further implies that the critical aggregation concentration is approximately related to $\Delta\mu_n^\circ$, as follows,

$$C_A \approx e^{+\beta\Delta\mu_n^\circ} \quad \text{or equivalently,} \quad \Delta\mu_n^\circ \approx RT\ln C_A. \tag{3}$$

Note that the latter expression is equivalent to the usual relation between the standard chemical potential of a micelle and the corresponding critical micelle concentration (C_A),[14–16] although here all concentrations are expressed in molar (rather than mole fraction) units. The above expressions pertain to any reasonable definition of C_A, including that at which $C_1 = C_n$ or $C_1 = \frac{1}{n}C_n$, as long as $n >> 1$ (as is typically the case for micelles).

If the critical micelle concentration is defined as that at which $C_1 = C_n = C_A$ then that implies that $C_A = \left(\frac{1}{nK_n}\right)^{\frac{1}{n-1}}$. Moreover, since the total monomer concentration C_T is the sum of the free and aggregated monomer concentrations, $C_T = C_1 + C_n = C_1[1+(C_1/C_A)^{n-1}]$. The second equality was obtained using $K_n = (C_n/n)/C_1^n$ to equate $C_n = n\,K_n\,C_1^n = C_1^n/C_A^{n-1}$. Thus, given C_A and n, one may predict C_T as a function of C_1, and then plot C_1 and $C_n = C_T - C_1$ as functions of C_T, which is how the dotted curves in Fig. 1D and Fig. 2 of the parent manuscript were generated for the formation of 12HD micelles.

If the aqueous solution also contains salt of concentration C_S (pertaining to the concentration of the neutral combination of cations and anions), then the chemical potentials of the free and aggregated monomers in the salt solution may be expressed as follows.

$$\mu_{1,S}^\circ = \mu_1^\circ + k_1 C_S \tag{4}$$

$$\mu_{n,S}^\circ = \mu_n^\circ + k_n C_S \tag{5}$$

The coefficients k_i, which are closely related to the so-called Setschenow (or Setchenov) constants,[15,17,18] quantify the influence of the salt on the chemical potentials of the free and aggregated surfactant molecules in the low salt concentration limit. By subtracting Eq. 4 from Eq. 5, we obtain the following difference between the micelle and monomer chemical potentials in the salt solution

(where $\Delta k = k_n - k_1$).

$$\Delta\mu^{\circ}_{n,S} = \Delta\mu^{\circ}_{n} + \Delta\mu^{\times}_{n,S} = \Delta\mu^{\circ}_{n} + \Delta k C_S \tag{6}$$

The last term in Eq. 6 may also be expressed as $\Delta k C_S = RT(\beta\Delta k C_S)$, where $\beta\Delta k C_S = \Delta k C_S / RT$ is a dimensionless quantity whose magnitude may safely be assumed to be much less than 1 (as long as the salt concentration is sufficiently low that $\Delta k C_S << RT$). In this limit, to first order in $\beta\Delta k C_S$, we may equate $\Delta k C_S = RT \ln(1 + \beta\Delta k C_S)$ and thus

$$\Delta\mu^{\circ}_{n,S} = RT \ln C_A + RT \ln(1 + \beta\Delta k C_S) = RT \ln[C_A(1 + \beta\Delta k C_S)] = RT \ln C_A^S \tag{7}$$

where the critical aggregate concentration in the presence of the salt solution, C_A^S, is related to that in the absence of salt, C_A, as follows.

$$C_A^S = C_A(1 + \beta\Delta k C_S) \tag{8}$$

This further implies that one may experimentally determine Δk from the measured influence of a salt on the critical aggregate concentration, where $\Delta C_A = C_A^S - C_A$,

$$\Delta k \approx RT \left(\frac{\Delta C_A}{C_A C_S} \right) \tag{9}$$

or equivalently

$$\Delta\mu^{\times}_{n,S} = \Delta k C_S \approx RT \left(\frac{\Delta C_A}{C_A} \right) \tag{10}$$

The above results may further be related to Wyman-Tanford theory, which links the aggregation equilibrium constant to the excess partitioning of salt (and water) to the free and aggregated surfactant hydration shells. Specifically, the Wyman-Tanford excess partition coefficient is defined as[19–22]

$$\Gamma = \left\langle n_W \left(\frac{n_S}{n_W} - \frac{N_S - n_S}{N_W - n_W} \right) \right\rangle \tag{11}$$

where N_i are the total number of molecules of type i in the system (where $i = S$ for salt and $i = W$ for water), and n_i are the corresponding number of molecules in the hydration shell of the surfactant. Note that Γ will be equal to zero if the local salt to water ratio in the surfactant hydration shell,

n_S/n_W, is equal to that far from the surfactant, $(N_S - n_S)/(N_W - n_W)$, and Γ will be positive when salt ions accumulate around the surfactant, such that $n_S/n_W > (N_S - n_S)/(N_W - n_W)$, and conversely Γ will be negative if salt ions are expelled from the surfactant hydration shell. Note that in the extreme expulsion limit $n_S = 0$ and thus $(N_S - n_S)/(N_W - n_W) = N_S/(N_W - n_W) > N_S/N_W$, as expulsion of salt from the surfactant hydration shell will increase the salt concentration in the surrounding solvent. It is also important to note that the above expression implies that when Γ is not equal to zero, its magnitude is expected to increase with increasing salt concentration, because both n_S/n_W and $(N_S - n_S)/(N_W - n_W)$ increase with increasing salt concentration.

Wymann-Tanford theory, combined with Eq. 10, yields the following relationship between the salt concentration derivative of $\ln K_n$ and the corresponding excess partition coefficients.

$$\frac{d \ln K_n}{d \ln C_S} = C_S \left(\frac{d \ln K_n}{dC_S} \right) = \frac{-nC_S}{RT} \left(\frac{d\Delta\mu^{\circ}_{n,S}}{dC_S} \right) = \frac{-n\Delta k C_S}{RT} = \Gamma_A - \Gamma_F \tag{12}$$

Note that Γ_A pertains to partitioning of salt to the hydration shell of the entire aggregate (micelle) containing n monomers, and Γ_F pertains to partitioning of the salt to the hydration shells of a collection of n free monomers, and thus the magnitudes of both Γ_A and Γ_F are expected to increase with increasing micelle size. Equations 10 and 12 imply that the measured salt-induced change in the critical micelle concentration may be used to experimentally determine $\Delta\Gamma = \Gamma_A - \Gamma_F$.

$$\Delta\Gamma = -n \left(\frac{\Delta C_A}{C_A} \right) = -n \left(\frac{C_S \Delta k}{RT} \right) = -n\beta\Delta\mu^{\times}_{n,S} \tag{13}$$

Thus, a salt-induced decrease in C_A implies that $\Gamma_A > \Gamma_F$, independent of the signs of Γ_A and/or Γ_F. In other words, a decrease in C_A may occur either when salt has a net affinity for both the free and aggregated surfactant or a net expulsion from both, as long as the salt ions have a greater affinity for the micelle than the free surfactant monomers.

4 Wyman-Tanford Partition Coefficient Bounds

The salt-induced changes in 12HD critical micelle concentration, C_A, have been used to directly determine that $\Delta\Gamma \approx 4.6$ in 0.25 M Na_2SO_4 and $\Delta\Gamma \approx 4.0$ in 2 M NaSCN, as described in the parent manuscript. Physically reasonable ranges of values for Γ_F and Γ_A in the two salt solutions may be

established by considering the following limiting scenarios: i) assume that the salts do not change the micelle chemical potential ii) assume that the salt concentration is the same in the hydration shells of the free surfactant monomers and micelles.

The first of the above two scenarios amounts to assuming that $\Gamma_A = 0$, in which case one would obtain $\Gamma_F \approx -4.6$ in 0.25 M Na_2SO_4 and $\Gamma_F \approx -4.0$ in 2 M NaSCN. The second scenario implies that $\frac{n_s}{n_w} - \frac{N_s - n_s}{N_w - n_w}$ is the same for the free and aggregated 12HD solutions, and thus that $\frac{\Gamma_A}{\Gamma_F} \approx \frac{\langle n_w \rangle_A}{\langle n_w \rangle_F}$. The latter ratio (which corresponds to the ratio of the number of water molecules in the hydration shell of the aggregated and free monomers) is estimated to be $\frac{\langle n_w \rangle_A}{\langle n_w \rangle_F} \approx 0.27$, obtained from the ratio of the areas of the OH band in the hydration shell spectra of the aggregated (micelle) and free monomers, corresponding to the dotted-black and solid-red OH bands in Fig. 1(B) of the parent manuscript. Thus, this second scenario would imply that in 0.25 M Na_2SO_4 $\Gamma_F \approx \frac{4.6}{0.27-1} \approx -6.3$ and thus $\Gamma_A \approx -1.7$, while in 2 M NaSCN $\Gamma_F \approx \frac{4.0}{0.27-1} \approx -5.5$ and thus $\Gamma_A \approx -1.5$.

Although the above two scenarios provide a physically reasonable range of Γ values, they do not necessarily represent firm upper and lower limits on the possible values of Γ. For example, our Raman-MCR spectra indicate that SCN^- penetrates more significantly into the hydration shell of the micelle than the free 12HD monomer, as evidenced by the surfactant correlated C≡N bands shown in Fig. S3. Specifically, the red-shifted C≡N band arising from SCN^- in the micelle hydration shell has a larger area than the blue-shifted C≡N band arising from the hydration shell of the free monomer (both of which have been normalized to pertain to the same 12HD concentration). This suggests $\frac{n_s}{n_w} - \frac{N_s - n_s}{N_w - n_w}$ has a larger (more positive or less negative) value in the hydration shell of the micelle than the free monomer, and thus in 2 M NaSCN our results are also consistent with $\Gamma_F > -4$ and $\Gamma_A \gtrsim 0$. On the other hand, our Raman-MCR of 12HD in 0.25 M Na_2SO_4 indicate that sulfate ions are strongly expelled from the hydration shell of a free 12HD monomer, thus implying that $n_s \approx 0$, and thus $\Gamma_F = -\left\langle \frac{n_W N_S}{N_W - n_W} \right\rangle \sim -12$ (obtained as described below), which is beyond the range of $-4.6 \geq \Gamma_F \geq -6.3$ established using the two scenarios described in the previous paragraph. Thus, in 0.25 M Na_2SO_4 the bounds on Γ_F may be extended to $-5 \geq \Gamma_F > -12$.

The lower bound of $\Gamma_F \approx -12$ for 12HD in Na_2SO_4 is obtained assuming that there are approximately $n_W \sim 63 \times 20 \sim 1260$ water molecules in the first hydration shells of 20 free 12HD molecules, and $N_W \sim (55/0.46) \times 20 \sim 2400$ when $[12HD]_T = C_A^S = 0.46$ M, and thus $N_S = N_W(0.25/55) \sim 11$ at a salt concentration of 0.25 M. The value of 63 ± 4 for the water

molecules in the hydration shell of a fully hydrated 12HD was obtained by performing a molecular dynamics simulation with two 12HD molecules and 400 water molecules at 20 °C (and 0.1 MPa), with TIP4P-2005 and OPLS-AA force fields and a first hydration-shell cut-off distance of 0.58 nm, for the water oxygen (Ow) atoms relative to any of the 12HD heavy atoms (C or O).

Note that the above Γ_i values also yield estimates of the k_i coefficients, since $k_i = -\left(\frac{RT}{nC_s}\right)\Gamma_i$. Thus, in 2 M NaSCN the above results imply that $k_1 \leq 0.34$ (kJ/mol M^{-1}) and k_n has a smaller magnitude and either a positive or negative sign. On the other hand, in 0.25 M Na_2SO_4 the above results imply that $2.4 \leq k_1 < 5.9$ (kJ/mol M^{-1}) and $0.2 \leq k_n < 3.6$ (kJ/mol M^{-1}).

References

[1] Lawton, W. H.; Sylvestre, E. A. *Technometrics* **1971**, *13*, 617–633.

[2] Perera, P.; Wyche, M.; Loethen, Y.; Ben-Amotz, D. *J. Am. Chem. Soc.* **2008**, *130*, 4576–4577.

[3] Gierszal, K. P.; Davis, J. G.; Hands, M. D.; Wilcox, D. S.; Slipchenko, L. V.; Ben-Amotz, D. *J. Phys. Chem. Lett.* **2011**, *2*, 2930–2933.

[4] Rankin, B. M.; Hands, M. D.; Wilcox, D. S.; Fega, K. R.; Slipchenko, L. V.; Ben-Amotz, D. *Faraday Discuss.* **2013**, *160*, 255–270.

[5] Mendes de Oliveira, D.; Ben-Amotz, D. *J. Phys. Chem. Lett.* **2019**, *10*, 2802–2805.

[6] Mendes de Oliveira, D.; Zukowski, S. R.; Palivec, V.; Hénin, J.; Seara, H. M.; Ben-Amotz, D.; Jungwirth, P.; Duboué-Dijon, E. *Phys. Chem. Chem. Phys,* **2020**, *22*, 24014–24027.

[7] Davis, J. G.; Gierszal, K. P.; Wang, P.; Ben-Amotz, D. *Nature* **2012**, *491*, 582–585.

[8] Wu, X. E.; Lu, W. J.; Streacker, L. M.; Ashbaugh, H. S.; Ben-Amotz, D. *J. Phys. Chem. Lett.* **2018**, *9*, 1012–1017.

[9] Wu, X. E.; Lu, W. J.; Streacker, L. M.; Ashbaugh, H. S.; Ben-Amotz, D. *Angew. Chem. Int. Ed.* **2018**, *57*, 15133–15137.

[10] Bredt, A. J.; Ben-Amotz, D. *Phys. Chem. Chem. Phys.* **2020**, *22*, 11724–11730.

[11] Long, J. A.; Rankin, B. M.; Ben-Amotz, D. *J. Am. Chem. Soc.* **2015**, *137*, 10809–10815.

[12] Fega, K. R.; Wilcox, A. S.; Ben-Amotz, D. *Appl. Spectrosc.* **2012**, *66*, 282–288.

[13] Ben-Amotz, D. *Understanding Physical Chemistry*; John Wiley and Sons: New York, 2014.

[14] Israelachvili, J. N. *Intermolecular and Surface Forces*, 2nd ed.; Academic Press: San Diego, 1991.

[15] Francisco, O. A.; Glor, H. M.; Khajehpour, M. *ChemPhysChem* **2020**, 484–493.

[16] Koroleva, S. V.; Victorov, A. I. *Langmuir* **2014**, *30*, 3387–3396.

[17] Koroleva, S. V.; Korchak, P.; Victorov, A. I. *J. Chem. Eng. Data* **2020**, *65*, 987–992.

[18] Long, F. A.; McDevit, W. F. *Chem. Rev.* **1952**, *51*, 119–169.

[19] Mochizuki, K.; Pattenaude, S. R.; Ben-Amotz, D. *J. Am. Chem. Soc.* **2016**, *138*, 9045–9048.

[20] Mondal, J.; Halverson, D.; Li, I. T.; Stirnemann, G.; Walker, G. C.; Berne, B. J. *Proc. Natl. Acad. Sci. U. S. A.* **2015**, *112*, 9270–9275.

[21] Wyman Jr, J. *Advances in protein chemistry*; Elsevier, 1964; Vol. 19; pp 223–286.

[22] Tanford, C. *J. Mol. Biol.* **1969**, *39*, 539–544.